INTERNATIONAL JOURNAL FOR NUMERICAL METHODS IN ENGINEERING, VOL. 24, 1801–1821 (1987)

CALCULATION OF FRACTURE MECHANICS PARAMETERS FOR AN ARBITRARY THREE-DIMENSIONAL CRACK, BY THE 'EQUIVALENT DOMAIN INTEGRAL' METHOD

G. P. NIKISHKOV* AND S. N. ATLURI†

Center for the Advancement of Computational Mechanics, Mail Code 0356, Georgia Institute of Technology, Atlanta, GA 30332, U.S.A.

SUMMARY

In this paper, an equivalent domain integral (EDI) method and the attendant numerical algorithms are presented for the computation of a near-crack-tip field parameter, the *vector* J_ε-integral, and its variation along the front of an arbitrary three-dimensional crack in a structural component. Account is taken of possible *non-elastic* strains present in the structure; in this case the near-tip J_ε-values may be significantly different from the far-field values J_Γ, especially under non-proportional loading.

INTRODUCTION

In the majority of practical cases, cracks in structures have arbitrary three-dimensional shapes and the crack faces may be non-planar. Therefore, we need methods to calculate fracture mechanics parameters for such cracks.

In general, linear or non-linear boundary value problems for a body with cracks can be solved only by some numerical method, e.g. the finite element method. Using the solutions thus obtained for the displacement and stress fields, it is possible to define the fracture mechanics parameters (such as the stress intensity factors $K_{\mathrm{I}}, K_{\mathrm{II}}, K_{\mathrm{III}}$ for the linear case, and the vector J_ε-integral in the elastic–plastic case).

Today the most general and useful way to predict the behaviour of a cracked body is through the use of the J-integral fracture criterion. Basic definitions and procedures for J-integral calculation, in some very general cases, were considered in References 1–6. But only one publication[7] contains the results of mixed mode three-dimensional calculations.

It is generally recognized that energetic methods of fracture parameter calculation have a higher rate of convergence to the hypothetical exact solution. For this reason, the virtual crack extension (VCE) method[4,5] and its earlier versions[8,9] are very attractive.

In this publication we present a further development of the VCE method, labelled here as the 'equivalent domain integral' (EDI) method, for J-integral calculation in a general three-dimensional static case, taking into account the non-elastic strains. The EDI method provides a new interpretation of the VCE technique and allows us to show the equivalence of an EDI calculated J-integral to crack tip parameter J_ε and to simplify the numerical procedure. The validity of the presented formulation is demonstrated by solving some three-dimensional mixed crack problems.

---

†Visiting Associate Professor. Permanent Address: Moscow Institute of Engineering Physics, Moscow, 115409 U.S.S.R.
*Regents' Professor & Director

0029–5981/87/091801–21$10.50

Received 8 August 1986
Revised 9 December 1986

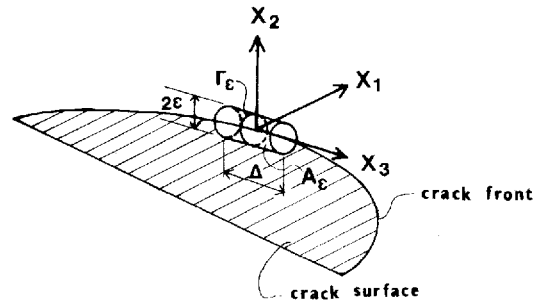

Figure 1. Nomenclature near the front of a three-dimensional crack

BASIC DEFINITION OF J-INTEGRAL

The J-integral, as a fracture mechanics parameter, was introduced by Cherepanov[10] and Rice.[11] According to Reference 12 the basic definition of J-integral components, as crack-tip parameters, is (see Figure 1) given by

$$J_k = \lim_{E \to 0} \int_{\Gamma_\varepsilon} \left[W n_k - \sigma_{ij} \frac{\partial u_i}{\partial x_k} n_j \right] \mathrm{d}\Gamma \tag{1}$$

Here W is the stress-work density, σ_{ij} are stresses, u_i are displacements, n_k are components of the unit normal vector to the surface of the tube at points on the contour Γ. In principle it is possible to define J_k in any co-ordinate system, but for the purpose of prediction of crack behaviour, it is more convenient to have a local crack front co-ordinate system x_1, x_2, x_3: x_1 is normal to the crack front and lies in the plane of the crack surface, x_2 is orthogonal to x_1 and the crack surface, and x_3 is tangential to the crack front and in the crack plane.

Let us introduce the equivalent definition of the near-tip J-integral along the surface of the tube:

$$J_k \Delta = \lim_{\substack{\varepsilon/\Delta \to 0 \\ \Delta \to 0}} \int_{A_\varepsilon} \left[W n_k - \sigma_{ij} \frac{\partial u_i}{\partial x_k} n_j \right] \mathrm{d}\Gamma, \quad k = 1, 2 \tag{2}$$

This definition is more convenient for numerical applications.

FRACTURE CRITERION AND CALCULATION OF STRESS INTENSITY FACTORS IN THE LINEAR CASE

The experimental data available to date, concerning the general mixed mode fracture, are not sufficient to establish the validity of any one particular fracture criterion. In terms of the J-integral the most evident criteria are[12]:

Criterion 1 (originating from the Griffith condition)

$$J_1 = J_c \tag{3}$$

Criterion 2

$$\sqrt{(J_1^2 + J_2^2)} = J_c \tag{4}$$

where J_c is some experimentally defined material constant. It is worthy of note that, in general, the quantities J_k as defined in equations (1) and (2) do not have any interpretation involving an

energy release rate: they are simply parameters that govern the severity of the crack-tip fields.

In the linear elastic case, it is possible to define stress intensity factors through the calculation of J_k. According to Reference 12 the relationships between the J-integral components and the stress intensity factors are

$$J_1 = \frac{1}{E^*}(K_{\mathrm{I}}^2 + K_{\mathrm{II}}^2) + \frac{1}{2\mu}K_{\mathrm{III}}^2 \tag{5a}$$

$$J_2 = -\frac{2}{E^*}K_{\mathrm{I}}K_{\mathrm{II}} \tag{5b}$$

Here

$$\mu = \frac{E}{2(1+\nu)} \tag{6}$$

$$E^* = \begin{cases} E/(1-\nu)^2 & \text{plane strain} \\ E & \text{plane stress} \end{cases} \tag{7}$$

and E, ν are the Young's modulus and the Poisson's ratio respectively. In Reference 12 it is proposed to define E^* as

$$E^* = \left[E\frac{1}{1-\nu^2} + \left(\frac{\nu}{1+\nu}\right)\frac{\varepsilon_{33}}{\varepsilon_{11}+\varepsilon_{22}} \right] \tag{8}$$

This expression leads to (7) for the cases of plane strain and plane stress respectively, and gives some kind of interpolation for any intermediate stress state. The strains $\varepsilon_{11}, \varepsilon_{22}, \varepsilon_{33}$ should be defined in the vicinity of crack front.

It is evident that it is impossible to define $K_{\mathrm{I}}, K_{\mathrm{II}}, K_{\mathrm{III}}$ from (5) alone. There are two possible ways to solve (5) to obtain the stress intensity factors.

The first approach is to add the expressions containing energy release rates $G_{\mathrm{I}}, G_{\mathrm{II}}$ and G_{III}:

$$J_1 = G_{\mathrm{I}} + G_{\mathrm{II}} + G_{\mathrm{III}} \tag{9}$$

$$G_{\mathrm{III}} = \frac{1}{2\mu}K_{\mathrm{III}}^2 \tag{10}$$

$$G_{\mathrm{III}}\Delta = \lim_{\substack{\varepsilon/\Delta\to 0 \\ \Delta\to 0}} \int_{A_\varepsilon} \left[W^{\mathrm{III}} n_1 - \sigma_{3j}\frac{\partial u_3}{\partial x_1} n_j \right] \mathrm{d}A \tag{11}$$

where W^{III} should be calculated by using strain and stress components $\varepsilon_{3j}, \sigma_{3j}$, in the crack-front co-ordinate system of Figure 1. Then the relation between stress intensity factors and J_1, J_2 and G_{III} is[13]

$$\begin{aligned} K_I &= \tfrac{1}{2}\sqrt{E^*}(\sqrt{(J_1 - J_2 - G_{\mathrm{III}})} + \sqrt{(J_1 + J_2 - G_{\mathrm{III}})}) \\ K_{\mathrm{II}} &= \tfrac{1}{2}\sqrt{E^*}(\sqrt{(J_1 - J_2 - G_{\mathrm{III}})} - \sqrt{(J_1 + J_2 - G_{\mathrm{III}})}) \\ K_{\mathrm{III}} &= \sqrt{(2\mu G_{\mathrm{III}})} \end{aligned} \tag{12}$$

Another way is through the decomposition of displacement and stress fields into symmetric and antisymmetric portions[6,14,15]

$$\{u\} = \{u^{\mathrm{I}}\} + \{u^{\mathrm{II}}\} + \{u^{\mathrm{III}}\} = \frac{1}{2}\begin{Bmatrix} u_1 + u_1' \\ u_2 - u_2' \\ u_3 + u_3' \end{Bmatrix} + \frac{1}{2}\begin{Bmatrix} u_1 - u_1' \\ u_2 + u_2' \\ 0 \end{Bmatrix} + \frac{1}{2}\begin{Bmatrix} 0 \\ 0 \\ u_3 - u_3' \end{Bmatrix} \tag{13}$$

$$\{\sigma\} = \{\sigma^{\mathrm{I}}\} + \{\sigma^{\mathrm{II}}\} + \{\sigma^{\mathrm{III}}\} = \frac{1}{2}\begin{bmatrix} \sigma_{11} + \sigma'_{11} \\ \sigma_{22} + \sigma'_{22} \\ \sigma_{33} + \sigma'_{33} \\ \sigma_{12} - \sigma'_{12} \\ \sigma_{23} - \sigma'_{23} \\ \sigma_{31} - \sigma'_{31} \end{bmatrix} + \frac{1}{2}\begin{bmatrix} \sigma_{11} - \sigma'_{11} \\ \sigma_{22} - \sigma'_{22} \\ 0 \\ \sigma_{12} + \sigma'_{12} \\ 0 \\ 0 \end{bmatrix} + \frac{1}{2}\begin{bmatrix} 0 \\ 0 \\ \sigma_{33} - \sigma'_{33} \\ 0 \\ \sigma_{23} + \sigma'_{23} \\ \sigma_{31} + \sigma'_{31} \end{bmatrix} \tag{14}$$

$$u'_i(x_1, x_2, x_3) = u_i(x_1, -x_2, x_3) \tag{15}$$

$$\sigma'_{ij}(x_1, x_2, x_3) = \sigma_{ij}(x_1, -x_2, x_3) \tag{16}$$

By using (13)–(14) and (2) it is possible to compute G_{I} and G_{II}:

$$G_{\mathrm{I}}\Delta = \lim_{\substack{\varepsilon/\Delta \to 0 \\ \Delta \to 0}} \int_{A_\varepsilon} \left(W^{\mathrm{I}} n_1 - \sigma^{\mathrm{I}}_{ij} \frac{\partial u^{\mathrm{I}}_i}{\partial x_1} n_j \right) \mathrm{d}A \tag{17}$$

$$G_{\mathrm{II}}\Delta = \lim_{\substack{\varepsilon/\Delta \to 0 \\ \Delta \to 0}} \int_{A_\varepsilon} \left(W^{\mathrm{II}} n_1 - \sigma^{\mathrm{II}}_{ij} \frac{\partial u^{\mathrm{II}}_i}{\partial x_1} n_j \right) \mathrm{d}\Gamma \tag{18}$$

G_{III} can be calculated from (11). The expressions for stress intensity factors become

$$\begin{aligned} K_{\mathrm{I}} &= \sqrt{(E^* G_{\mathrm{I}})} \\ K_{\mathrm{II}} &= \sqrt{(E^* G_{\mathrm{II}})} \\ K_{\mathrm{III}} &= \sqrt{(2\mu G_{\mathrm{III}})} \end{aligned} \tag{19}$$

TRANSFORMATION OF DISPLACEMENTS, STRAINS AND STRESSES TO THE CRACK FRONT CO-ORDINATE SYSTEM

We can simplify many developments if this transformation is performed prior to the calculation of J- and G-components. Let X_1, X_2, X_3 be a global Cartesian co-ordinate system; and x_1, x_2, x_3 be the crack-front co-ordinate system for a particular point along the crack front. For the definition of a crack-front co-ordinate system at any point, it is sufficient to have the direction cosines for a unit vector along x_1,

$$X_p = \{X_{p1}, X_{p2}, X_{p3}\} \tag{20}$$

and for a unit vector along x_3

$$Z_p = \{Z_{p1}, Z_{p2}, Z_{p3}\} \tag{21}$$

Then it is easy to define the orientation of x_2 as

$$Y_p = Z_p X X_p \tag{22}$$

$$\begin{aligned} Y_{p1} &= Z_{p2} X_{p3} - Z_{p3} X_{p2} \\ Y_{p2} &= Z_{p3} X_{p1} - Z_{p1} X_{p3} \\ Y_{p3} &= X_{p1} X_{p2} - Z_{p2} X_{p1} \end{aligned} \tag{23}$$

We define the coefficients of a transformation matrix a_{ij} as

$$\begin{aligned} a_{11} &= X_{p1} & a_{12} &= X_{p2} & a_{13} &= X_{p3} \\ a_{21} &= Y_{p1} & a_{22} &= Y_{p2} & a_{23} &= Y_{p3} \\ a_{31} &= Z_{p1} & a_{32} &= Z_{p2} & a_{33} &= Z_{p3} \end{aligned} \tag{24}$$

The transformation of co-ordinates, displacements, strains and stresses can be done as follows:

$$x_i = a_{ij} X_j \tag{25}$$

$$u_i = a_{ij} u_i^{\mathrm{g}} \tag{26}$$

$$\varepsilon_{ij} = a_{ip} a_{jq} \varepsilon_{pq}^{\mathrm{g}} \tag{27}$$

$$\sigma_{ij} = a_{ip} a_{jq} \sigma_{pq}^{\mathrm{g}} \tag{28}$$

Here the superscript g stands for the values in the global co-ordinate system.

EDI-TECHNIQUE FOR J_1, J_2 AND G_{III} CALCULATION

After a point by point co-ordinate transformation (25), the crack front is straight. Let us consider the segment of crack front and the volume around this segment inside the disk, as shown in Figure 2. (V is the volume of the disk, V_ε is the volume of small tube around the crack front segment, A is the cylindrical surface of V; A_ε is the cylindrical surface of V_ε and A_1, A_2 are side surfaces of V).

Then, in general, we can redefine the near-tip parameters J_k and G_{III} as

$$J_k f = -\int_{A-A_\varepsilon} \left(W n_k - \sigma_{ij} \frac{\partial u_i}{\partial x_k} n_j \right) s \, \mathrm{d}A \tag{29}$$

$$G_{\mathrm{III}} f = -\int_{A \quad A_\varepsilon} \left(W^{\mathrm{III}} n_1 - \sigma_{3j} \frac{\partial u_3}{\partial x_1} n_j \right) s \, \mathrm{d}A \tag{30}$$

Here $s = s(x_1, x_2, x_3)$ is an arbitrary but continuous function which is equal to zero on A, and non-zero on A_ε (as shown on Figure 2); and f is the area under the s-function curve along the segment of the crack-front under consideration (see Figure 2).

Using the divergence theorem, we have the following representation of J_k:

$$J_k f = -\int_{V-V_\varepsilon} \left(W \frac{\partial s}{\partial x_k} - \sigma_{ij} \frac{\partial u_i}{\partial x_k} \frac{\partial s}{\partial x_j} \right) \mathrm{d}v - \int_{V-V_\varepsilon} \left[\frac{\partial w}{\partial x_k} - \frac{\partial}{\partial x_j} \left(\sigma_{ij} \frac{\partial u_i}{\partial x_k} \right) \right] s \, \mathrm{d}v$$
$$+ \int_{A_1 + A_2} \left(W n_k - \sigma_{ij} \frac{\partial u_i}{\partial x_k} n_j \right) s \, \mathrm{d}A \tag{31}$$
$$k = 1, 2$$

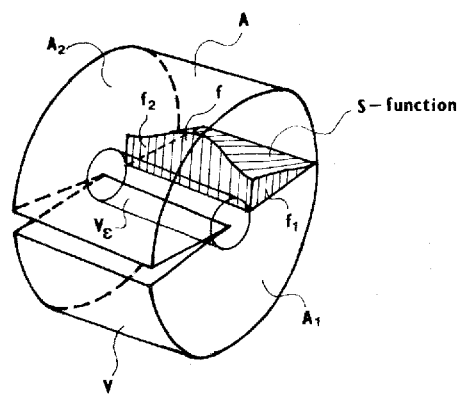

Figure 2. Definition of the s-function for a segment of the crack front

This expression represents a further variant of the VCE method,[4,5,8,9] but the elimination of the actual process of virtual crack extension during the development of (31) allows us to use any s-function for the calculation of J_k. Thus, we have a new and computationally more appealing interpretation of the VCE approach.

In the case of the presence of non-elastic (thermal and plastic) deformations we can define W as

$$W = \int \sigma_{ij} \, \mathrm{d}\varepsilon_{ij}^{\mathrm{ep}} \tag{32}$$

$$\varepsilon = \varepsilon_{ij}^{\mathrm{e}} + \varepsilon_{ij}^{\mathrm{p}} + \varepsilon_{ij}^{\mathrm{t}} \tag{33}$$

where $\varepsilon_{ij}^{\mathrm{e}}, \varepsilon_{ij}^{\mathrm{p}}$ and $\varepsilon_{ij}^{\mathrm{t}}$ and the elastic, plastic and thermal parts of the strains.

Assuming that the stresses have an elastic potential, i.e.

$$\sigma_{ij} = \frac{\partial w^{\mathrm{e}}}{\partial \varepsilon_{ij}^{\mathrm{e}}} \tag{34}$$

the second term of (31) can have the form

$$\begin{aligned}(J_k f)_2 &= -\int_{V-V_\varepsilon} \left(\frac{\partial w}{\partial x_k} - \sigma_{ij} \frac{\partial \varepsilon_{ij}}{\partial x_k} \right) s \, \mathrm{d}v \\ &= -\int_{V-V_\varepsilon} \left(\frac{\partial w^{\mathrm{p}}}{\partial x_k} - \sigma_{ij} \frac{\partial \varepsilon_{ij}^{\mathrm{pt}}}{\partial x_k} \right) s \, \mathrm{d}v \end{aligned} \tag{35}$$

Here we used equilibrium equations (in the absence of body forces), and introduced the definitions

$$W^{\mathrm{p}} = \int \sigma_{ij} \, \mathrm{d}\varepsilon_{ij}^{\mathrm{p}} \tag{36}$$

$$\varepsilon_{ij}^{\mathrm{pt}} = \varepsilon_{ij}^{\mathrm{p}} + \varepsilon_{ij}^{\mathrm{t}} \tag{37}$$

It is evident that, in the absence of non-elastic strains, the second term of (31) is equal to zero. If the s-function is equal to zero on faces A_1 and A_2, then the third term of (31) will be equal to zero as well.

Considering G_{III} for the linear elastic case (in the absence of body forces), we can have from equation (30),

$$\begin{aligned} G_{\mathrm{III}} f = &-\int_{V-V_\varepsilon} \left(W^{\mathrm{III}} \frac{\partial s}{\partial x_1} - \sigma_{3j} \frac{\partial u_3}{\partial x_1} \frac{\partial s}{\partial x_j} \right) \mathrm{d}V - \int_{V-V_\varepsilon} \sigma_{3j} \frac{\partial \varepsilon_{ij}^{\mathrm{t}}}{\partial x_1} s \, \mathrm{d}V \\ &+ \int_{A_1+A_2} \left(W^{\mathrm{III}} n_1 - \sigma_{3j} \frac{\partial u_3}{\partial x_1} n_j \right) s \, \mathrm{d}A \end{aligned} \tag{38}$$

The third term of (31) and (38) can be simplified if the faces A_1 and A_2 are orthogonal to the crack front ($n_1 = n_2 = 0$ on A_1 and A_2).

Again, in equation (38), the second term is equal to zero if $\varepsilon_{ij}^{\mathrm{t}} = 0$ and the third term is absent if $s = 0$ on A_1 and A_2.

We note that the 'equivalent domain integral' algorithms analogous to those in (31) can be developed directly for the energy-release rate quantities G_{I} and G_{II} as defined in (17) and (18) also.

FINITE ELEMENT PROCEDURE

We assume that the boundary value problem is solved by means of a finite element method, using 20-node quadratic brick type elements. The typical disk around the crack front segment

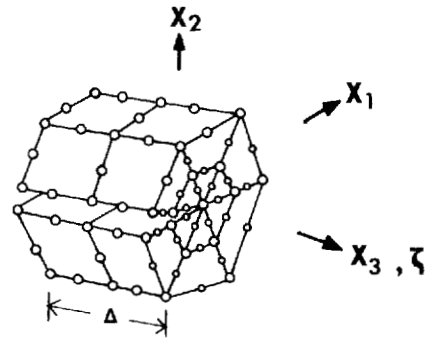

Figure 3. Details of the finite element mesh near a segment of the crack front

is shown in Figure 3. Usually because of mesh restrictions in the three-dimensional case, it is possible to have only 1 or 2 elements in the disk in the x_3-direction and say 1 to 3 elements in the radial direction.

Using 20-node elements we have the displacements at all nodes, and precise enough values of strains and stresses at the $2 \times 2 \times 2$ Gauss integration points.[16]

CHOICE OF s-FUNCTION

It is natural to use a parametric representation of function s inside any element

$$s = N^I s^I \qquad (I = 1 \ldots 20) \tag{39}$$

where $N^I = N^I(\xi, \eta, \zeta)$ are quadratic shape functions and I is the node number. We suppose summation over repeated indices. Then the s-function should be defined in terms of (39) by using 1 or 2 elements in the x_3-direction for the crack front disk. Usually it is not useful to have an s-function more complicated than a linear function in the radial direction. Several simple s-functions are presented in Figure 4.

(a) The disk has two elements each in the x_1 and x_3-directions respectively. The function s can be defined on the small tube of radius ε, for both the elements along x_3 (ζ being the natural

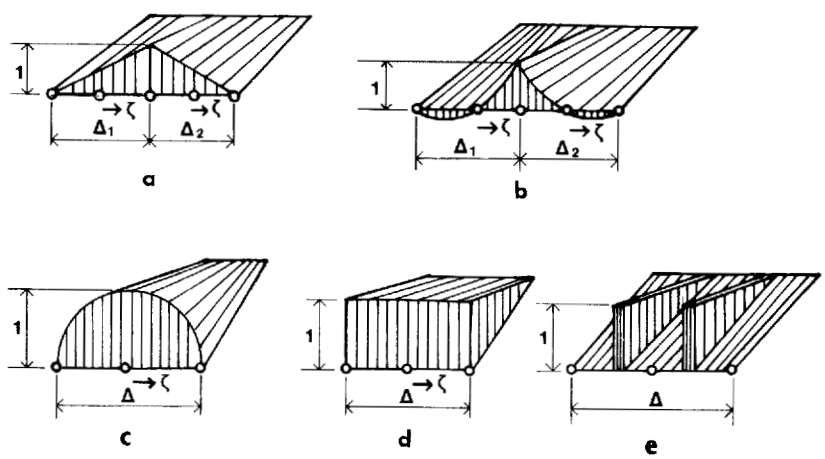

Figure 4. Definitions of several alternate s-functions

co-ordinate along the crack-front segment), as

$$\text{El. 1}: s = \tfrac{1}{2}(1+\zeta)$$
$$\text{El. 2}: s = \tfrac{1}{2}(1-\zeta)$$

The area under the s-function curve along the meridian of the surface of the small tube or on the crack front ($\varepsilon = 0$) is equal to

$$f = \tfrac{1}{2}(\Delta_1 + \Delta_2)$$

(b)
$$\text{El. 1}: s = \tfrac{1}{2}(\zeta^2 + \zeta)$$
$$\text{El. 2}: s = \tfrac{1}{2}(\zeta^2 - \zeta)$$
$$f = \tfrac{1}{3} + (\Delta_1 + \Delta_2)$$

(c)
$$s = (1 - \zeta^2)$$
$$f = \tfrac{2}{3}\Delta$$

(d)
$$s = 1$$
$$f = \Delta$$

(e) Figure 4(e) shows the possibility of carrying out the integrations involved in equation (31) along the two planes containing the integration (Gauss-quadrature) points only. The integration can be done precisely as in case (d), but dividing the results into two parts, leads to

$$s = 1$$
$$f = \frac{\Delta}{2}$$

Assuming an s-function that is linear in the r-direction we have its value for a particular point:

$$s = s_0 \frac{r - r_\varepsilon}{r_f - r_\varepsilon}$$

where s_0 is the value of the s-function at the point $r = r_\varepsilon$, r is the distance of the point in question from the surface of the small tube, r_ε is the radius of the small tube, r_f is the outer radius of the

Table I

Case	s-function on crack front	f	s-values at nodes														
			1	2	3	4	5	6	9	10	11	13	14	15	16	17	18
a	$\frac{1}{2}(1+\zeta)$	$\frac{1}{2}(\Delta_1+\Delta_2)$	1	0·75	0	0	0	0·75	0·5	0	0	0	0	0	0	0	0
	$\frac{1}{2}(1-\zeta)$		0	0	0	0	0	0	0·5	0	0	1	0·75	0	0	0	0·75
b	$\frac{1}{2}(\zeta^2+\zeta)$	$\frac{1}{3}(\Delta_1+\Delta_2)$	1	0·75	0	0	0	0·75	0	0	0	0	0	0	0	0	0
	$\frac{1}{2}(\zeta^2-\zeta)$		0	0	0	0	0	0		0	0	1	0·75	0	0	0	0·75
c	$1-\zeta^2$	$\frac{2}{3}\Delta$	0	0	0	0	0	0	1	0	0	0	0	0	0	0	0
d	1	Δ	1	1	0	0	0	0·75	1	0	0	1	0·75	0	0	0	0·75
e	1	$\frac{\Delta}{2}$	1	0·75	0	0	0	0·75	1	0	0	1	0·75	0	0	0	0·75

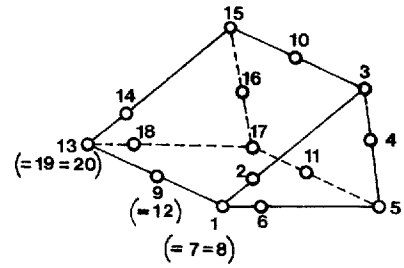

Figure 5. A degenerate quarter-point element spanning a segment of the crack front

crack-front disk of Figure 3. In practice it is often useful to have one element in the r-direction for the disk and to employ degenerate quarter-point singular elements around the crack tip. In this case it is very simple to define the s-function according to Table I and Figure 5. Note that cases (b), (c) were considered by the authors of References 4 and 5 in the context of node shifting, while the s-function types (a), (d), (e), are introduced here for the first time. Here the calculation of the area under the s-function curve along the crack-front segment, f, became possible, in a very simple manner, because of the previous co-ordinate transformation.

FIRST TERM OF J_k

Using the parametric representation of displacements

$$u_i = N^J u_i^J \tag{40}$$

where i is the direction of the crack-front co-ordinate system and the superscript J is the node number, it is possible to have such an expression for the calculation of the first term of the J-integral of equation (31):

$$(J_k f)_1 = -\int_{-1}^{1}\int_{-1}^{1}\int_{-1}^{1}\left(W\frac{\partial N^{\mathrm{L}}}{\partial x_k}s^{\mathrm{L}} - \sigma_{ij}\frac{\partial N^{\mathrm{M}}}{\partial x_k}\frac{\partial N^{\mathrm{L}}}{\partial x_j}u_i^{\mathrm{M}}s^{\mathrm{L}}\right)\det(j)\,\mathrm{d}\xi\,\mathrm{d}\eta\,\mathrm{d}\zeta \tag{41}$$

where $\det(j)$ is the determinant of the Jacobi matrix, and the superscripts L and M refer to node numbers. An effective procedure for computing J_k with several types of s-functions consists of a separate $2 \times 2 \times 2$ integration of the expression

$$R^{\mathrm{L}} = -\int_{-1}^{1}\int_{-1}^{1}\int_{-1}^{1}\left(W\frac{\partial N^{\mathrm{L}}}{\partial x_k} - \sigma_{ij}\frac{\partial N^{\mathrm{M}}}{\partial x_k}\frac{\partial N^{\mathrm{L}}}{\partial x_i}u_i^{\mathrm{M}}\right)\det(j)\,\mathrm{d}\xi\,\mathrm{d}\eta\,\mathrm{d}\zeta \tag{42}$$

and defining a scalar product

$$(J_k f)_1 = R^{\mathrm{L}} s^{\mathrm{L}} \tag{43}$$

SECOND TERM OF J_k

The main difficulty in integrating (35) arises from the fact that we know precise enough values of strain energy density and strain only at the $2 \times 2 \times 2$ Gauss Integration points.[16] A possible way of integrating the derivative of such functions is to obtain the derivative at the centre of the element and to perform a one-point integration.

Consider a 20-node element (Figure 6) in the local co-ordinate system ξ_i

$$\xi_1 = \xi, \quad \xi_2 = \eta, \quad \xi_3 = \zeta$$

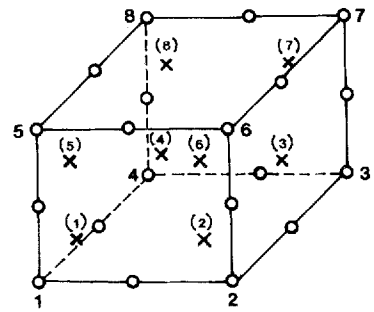

Figure 6. Nomenclature for a 20-node finite element, with (2 × 2 × 2) integration points

Let us thus assume that we know the values of the function F only at the integration points as $F^{(J)}$. Using a parametric representation, it is possible to write

$$F^{(J)} = L^{I(J)} F^I \tag{44}$$

where F^I are unknown values of F at corner nodes $1 \ldots 8$, L^I are linear shape functions for corner nodes, $L^{I(J)}$ are values of shape functions at integration points (J).

The inversion of (44) gives

$$F^I = (L^{I(J)})^{-1} F^{(J)} \tag{45}$$

The coefficients of the extrapolation matrix $(L^{I(J)})^{-1}$ are

$$(L^{I(J)})^{-1} \begin{bmatrix} A & B & C & B & B & C & D & C \\ & A & B & C & C & B & C & D \\ & & A & B & D & C & B & C \\ & & & A & C & D & C & B \\ & & & & A & B & C & B \\ & & & & & A & B & C \\ & & & & & & A & B \\ & & & & & & & A \end{bmatrix} \tag{46}$$

$$A = \frac{5+3\sqrt{3}}{4}, \quad B = -\frac{\sqrt{3}+1}{4}, \quad C = \frac{\sqrt{3}-1}{4}, \quad D = \frac{5-3\sqrt{3}}{4} \tag{47}$$

Now, from (45) we can calculate the derivative at the centre of the element:

$$\frac{\partial F}{\partial x_k} = \frac{\partial L^I}{\partial x_k} (L^{I(J)})^{-1} F^{(J)} \tag{48}$$

where the derivatives $\partial L^I / \partial x_k$ should be calculated for $\xi = \eta = \zeta = 0$.

THIRD TERM OF J_k OF EQUATION (31)

First, note that this term vanishes if $s = 0$ on A_1 and A_2. For simplicity consider the disk with A_1 and A_2 orthogonal to the crack-front segment. Then

$$\begin{aligned} &n_1 = n_2 = 0, \quad && n_3 = 1 \quad && \text{on } A_1 \\ &n_1 = n_2 = 0, \quad && n_3 = -1 \quad && \text{on } A_2 \end{aligned}$$

$$(J_k f)_3 = -\int_{A_1 + A_2} \sigma_{i3} \frac{\partial u_i}{\partial x_k} n_3 s \, \mathrm{d}A \tag{49}$$

If $A_1 = A_2$

$$(J_k f)_3 = -\int_{A_1} \Delta\left(\sigma_{i3}\frac{\partial u_i}{\partial x_k}\right) s\,\mathrm{d}A \tag{50}$$

where

$$\Delta(F) = (F)_{A_1} - (F)_{A_2}$$

Assuming that every function is linear in the x_3-direction and using the values of functions at integration points $\zeta = \pm(1/\sqrt{3})$, it is possible to define ΔF as

$$\Delta F = \sqrt{3}\left(F\left(\zeta = \frac{1}{\sqrt{3}}\right) - \left(\zeta = -\frac{1}{\sqrt{3}}\right)\right)$$

Then

$$(J_k f)_3 = -\int_{-1}^{1}\int_{1}^{1} \sqrt{3}\Delta\left(\sigma_{i3}\frac{\partial u_i}{\partial x_k}\right)^{(\mathrm{T})} s\,\mathrm{d}\xi\,\mathrm{d}\eta \tag{51}$$

where

$$\Delta F^{(\mathrm{T})} = F\left(\zeta = \frac{1}{\sqrt{3}}\right) - F\left(\zeta = -\frac{1}{\sqrt{3}}\right)$$

The integration (51) can be applied to the s-function of Figure 4(d). It is not possible to use (51) in the case of Figure 4(e). But if the diameter of the crack front disk is small compared to the crack depth, it is possible to neglect the third and second terms of J_k.

Here we consider several problems to illustrate the use of the above described algorithms.

PROBLEM 1. A CYLINDER WITH AN INNER CIRCULAR CRACK, SUBJECTED TO REMOTE TENSION

The problem is shown in Figure 7, the geometrical details being as follows.

$$(A/R = 0{\cdot}2)$$

Mesh: fifty-six 20-node elements, and 363 nodes (Figure 8). According to Reference 12 the

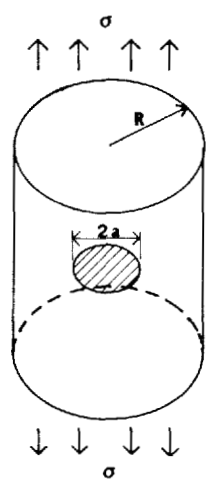

Figure 7. Mode-I problems of a penny-shaped crack in a tension-rod

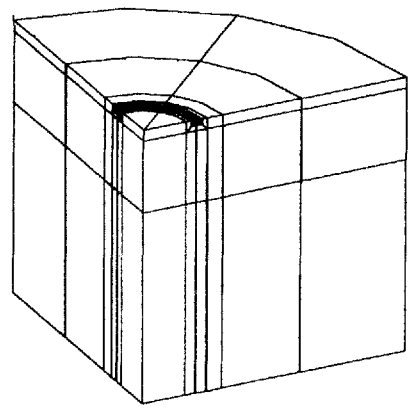

Figure 8. Finite element mesh for the problem of Figure 7

Table II

s-function	K_I	$\delta\%$
a	1·002	−0·2
b	1·010	0·5
c	0·998	−0·7
d	1·002	−0·2
e	1·002	−0·2

solution is

$$\bar{K}_I = K_I/(2\sigma\sqrt{a/\pi}) = 1{\cdot}005$$

Results and errors δ, obtained using different s-functions, are given in Table II.

This problem is a two-dimensional one, but it provides a test for the influence of the s-functions. The results obtained indicate that, for geometric modelling, it is possible to use only two layers of elements in the angular direction for a 90° segment of the crack front, for a problem of this type.

PROBLEM 2. A PLATE WITH A SEMI-ELLIPTICAL SURFACE CRACK, SUBJECT TO REMOTE TENSION

The problem is shown in Figure 9, the geometric details being

$$a/c = 0{\cdot}5$$
$$a/t = 0{\cdot}25$$

Mesh: One hundred and six 20-node elements, with 626 nodes (Figure 10). The comparison of results with the benchmark solution[17] is shown in Figure 11 for the normalized stress intensity factor

$$\bar{K}_I = K_I \Big/ \left(\frac{\sigma\sqrt{\pi a}}{\phi}\right)$$

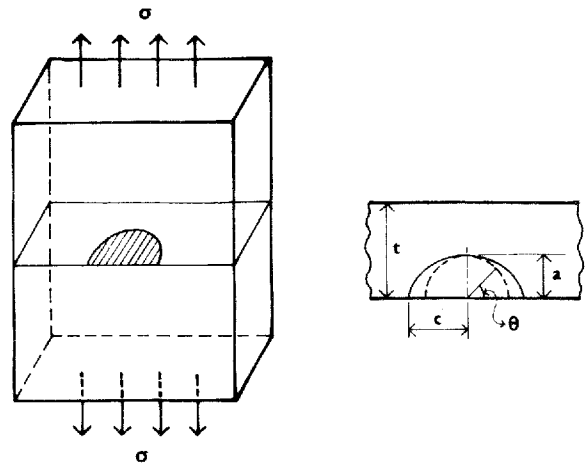

Figure 9. Schematic of the Mode I problem of a surface crack in a tension plate

Here ϕ is the complete elliptical integral of the second kind

$$\phi = \int_0^{\pi/2} \left(\frac{a^2}{c^2} \cos^2 \theta + \sin^2 \theta \right)^{1/2} d\theta$$

$$\phi = \left[1 + 1{\cdot}464 \left(\frac{a}{c} \right)^{1{\cdot}65} \right]^{1/2}$$

The maximum relative error in the present computations is 3·5 per cent.

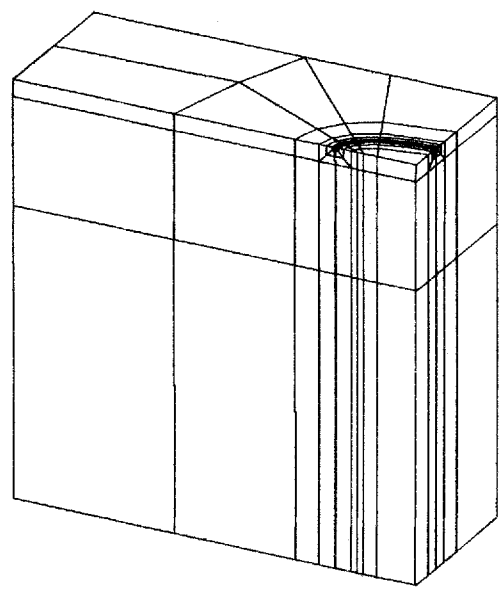

Figure 10. Finite element mesh for the problem of Figure 9

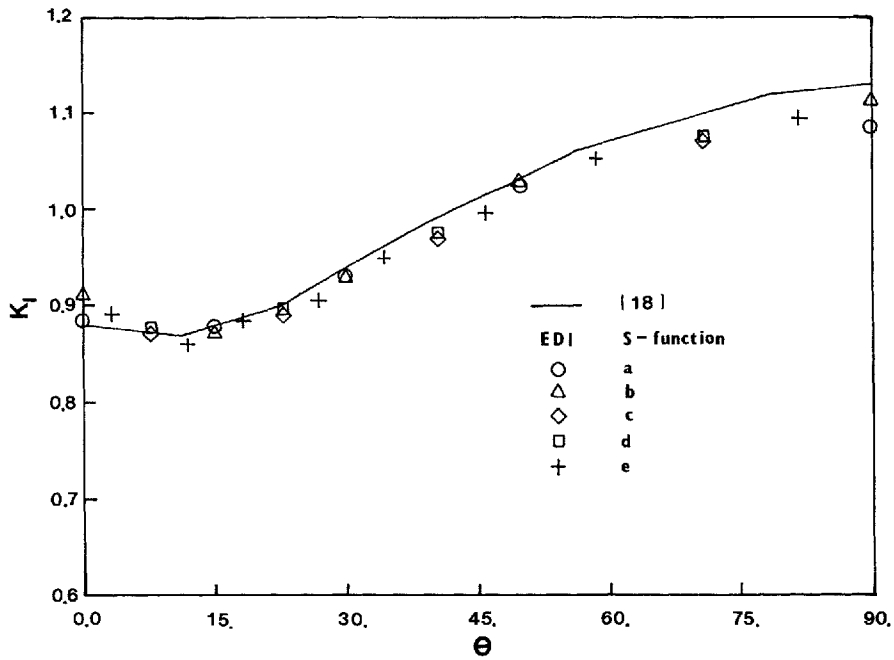

Figure 11. Results for normalized K_I for the problems of Figure 9, with different s-functions

PROBLEM 3. CALCULATION OF STRESS INTENSITY FACTORS FOR AN INCLINED CIRCULAR CRACK UNDER REMOTE TENSILE LOADING

To demonstrate the validity of the proposed procedures, the stress intensity factors for an embedded inclined circular crack under remote tensile loading are calculated (Figure 12). For the infinite body, the analytical solution was given in Reference 12. For $\alpha = 30$,

$$K_I = \frac{3}{2}\sigma\sqrt{\frac{\bar{a}}{\pi}}$$

$$K_{II} = \frac{\sqrt{3}}{2}\sigma\sqrt{\frac{\bar{a}}{\pi}}\cos\theta \tag{52}$$

$$K_{III} = \frac{\sqrt{3}}{2}\sigma\sqrt{\frac{\bar{a}}{\pi}}\sin\theta$$

$$J_1 = \frac{1+\nu}{E}\sigma^2\frac{a}{\pi}\frac{3}{4}[(1-\nu)(3+\cos^2\theta)+\sin^2\theta]$$

$$J_2 = -\frac{1-\nu^2}{E}\sigma^2\frac{a}{\pi}\frac{3\sqrt{3}}{2}\cos\theta \tag{53}$$

$$G_{III} = \frac{1+\nu}{E}\sigma^2\frac{a}{\pi}\frac{3}{4}\sin^2\theta$$

where θ is the angle for a particular point on the crack front.

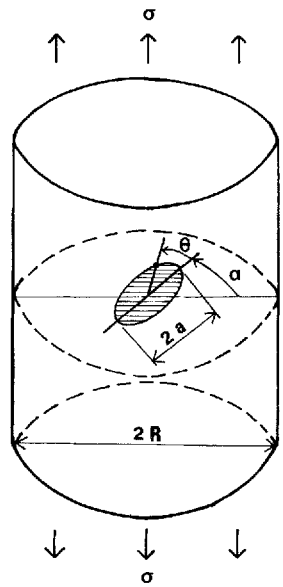

Figure 12. Schematic of an inclined penny-shaped crack in a tension rod

The finite element mesh is shown in Figure 13. It consists of 178 elements and 883 nodes. The mesh was created by rotating the two-dimensional mesh around the axis of the cylinder and then by rotating the region near the crack around the perpendicular axis.

It was assumed that $a/R = 0{\cdot}1$ and $\nu = 0{\cdot}3$. The size of the smallest element around the crack

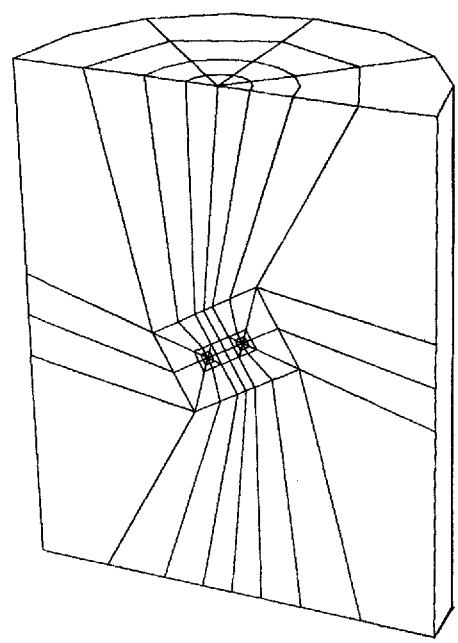

Figure 13. Finite element mesh for the problem of Figure 12

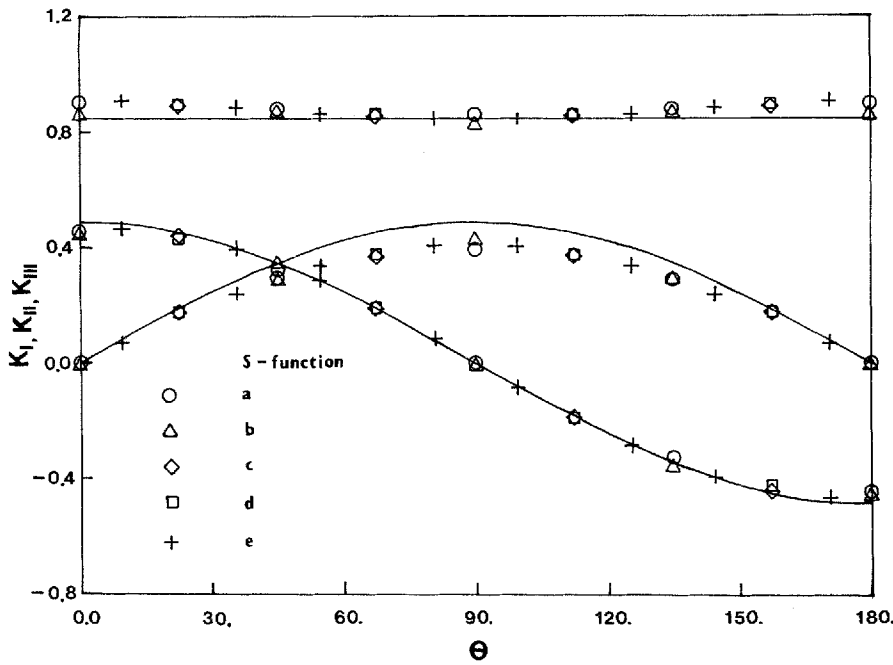

Figure 14. Results for normalized values of K_I, K_{II} and K_{III}, as obtained from the computed J_1, J_2 and G_{III}, for different s-functions

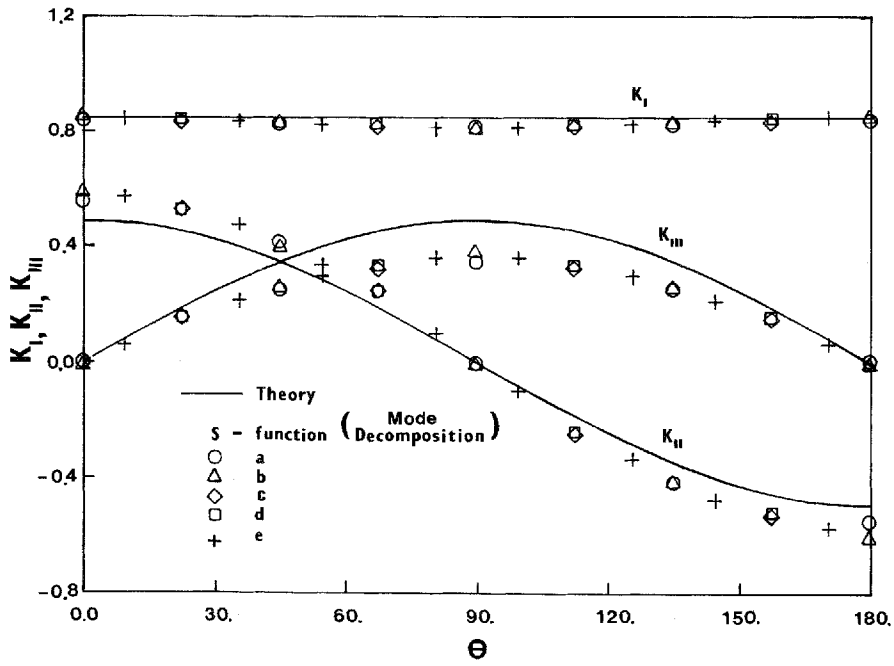

Figure 15. Results for normalized values of K_I, K_{II} and K_{III}, as obtained from the mode-decomposition method

front is 0·05 of the crack radius. The elements nearest to the crack front were used for the calculation of J and G components. The results for K_I, K_{II} and K_{III} normalized by $\sigma\sqrt{a}$ are shown in Figure 14, as obtained from the computed values for J_1, J_2, and G_{III}. The results for K_I, K_{II}, and K_{III}, normalized by $\sigma\sqrt{a}$, as obtained from the mode-decomposition method, are shown in Figure 15.

For the finite element mesh used (only four layers of elements for a 180° segment in the circular direction) the results are good. To our surprise even the s-function 'e' gave acceptable values. From these results it is possible to conclude that functions (a), (c), (e) should be used in practice. The use of these s-functions gives us values of the stress intensity factor for different points of the crack front (5 points for one element layer) of acceptable accuracy.

PROBLEM 4. SOLUTION FOR K_I, K_{II}, K_{III} FOR A SEMI-ELLIPTICAL SURFACE CRACK IN A CANTILEVER BEAM

The problem is shown in Figure 16, with

$$a/c = 0{\cdot}5$$
$$a/t = 0{\cdot}25$$
$$w = h$$
$$c/w = 0{\cdot}4$$

The finite element mesh (Figure 17) consists of 212 elements and 1165 nodes. It was composed of two blocks, as presented in Figure 10.

Results are shown in Figures 18–20 for the normalized stress intensity factors

$$\bar{K}_I = K_I \Big/ \left(\frac{\sigma_{max}\sqrt{\pi a}}{\phi} \right)$$

$$\bar{K}_{II} = K_{II} \Big/ \left(\frac{\tau\sqrt{\pi a}}{\phi} \right)$$

$$\bar{K}_{III} \Big/ \left(\frac{\tau\sqrt{\pi a}}{\phi} \right)$$

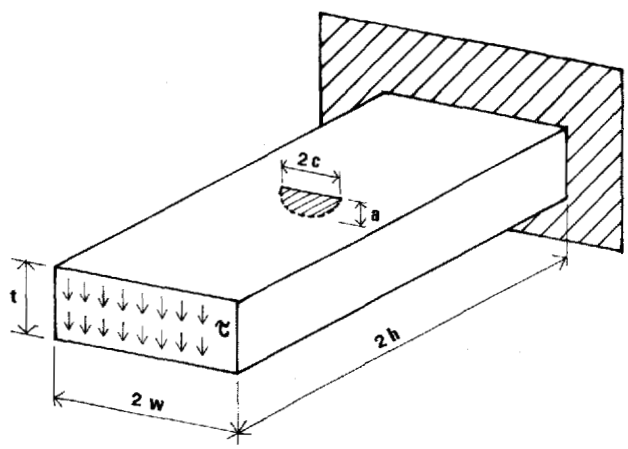

Figure 16. Schematic of a tip-loaded cantilever beam with a semi-elliptical surface flaw

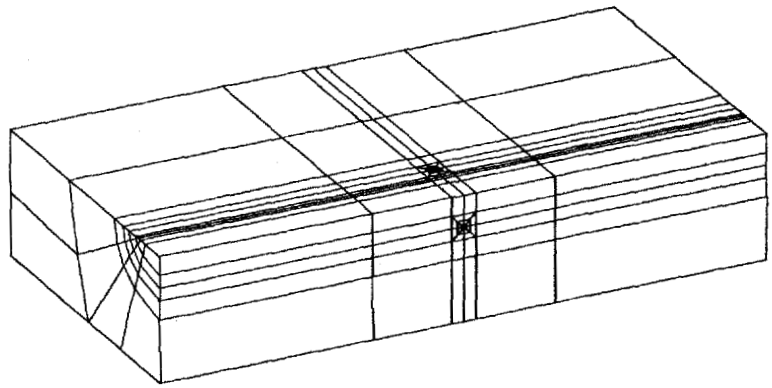

Figure 17. Finite element mesh for the problem of Figure 16

where σ_{max} is the maximum normal stress in the uncracked cross section, τ is average shear stress in the uncracked cross section and ϕ is the elliptical integral.

In Figure 18, K_1 is compared with the Benchmark solution.[17] In Figures 19–21, the results of Reference 7 are used for comparison. Figure 21 shows the EDI results on the basis of decomposed displacement stress fields. The dashed line represents the stress intensity factors defined from the displacement field and extrapolated to the crack front

$$K = 2K^{(1)} - K^{(2)}$$

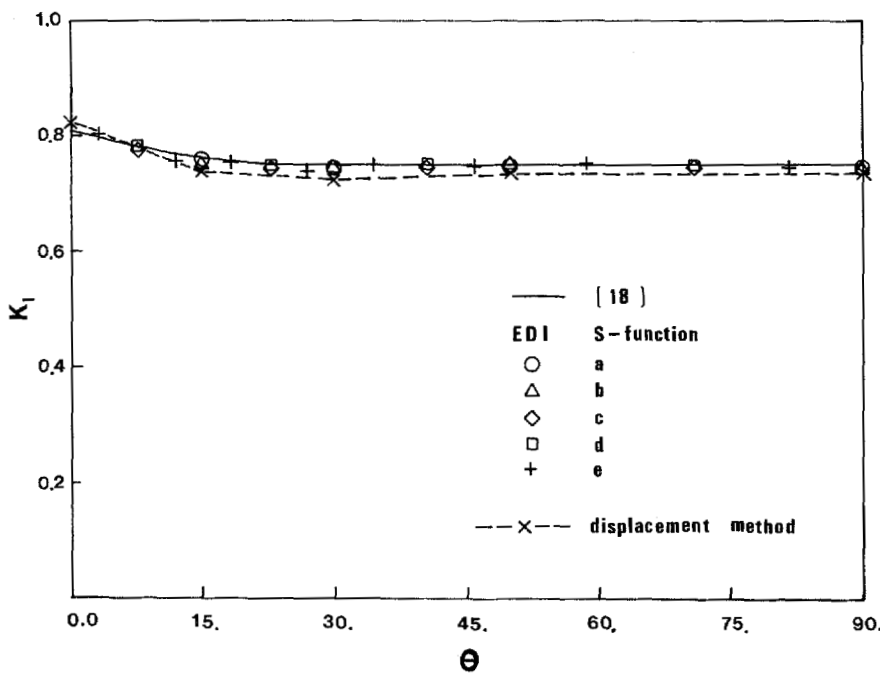

Figure 18. Results for normalized K_1 for the problem of Figure 16

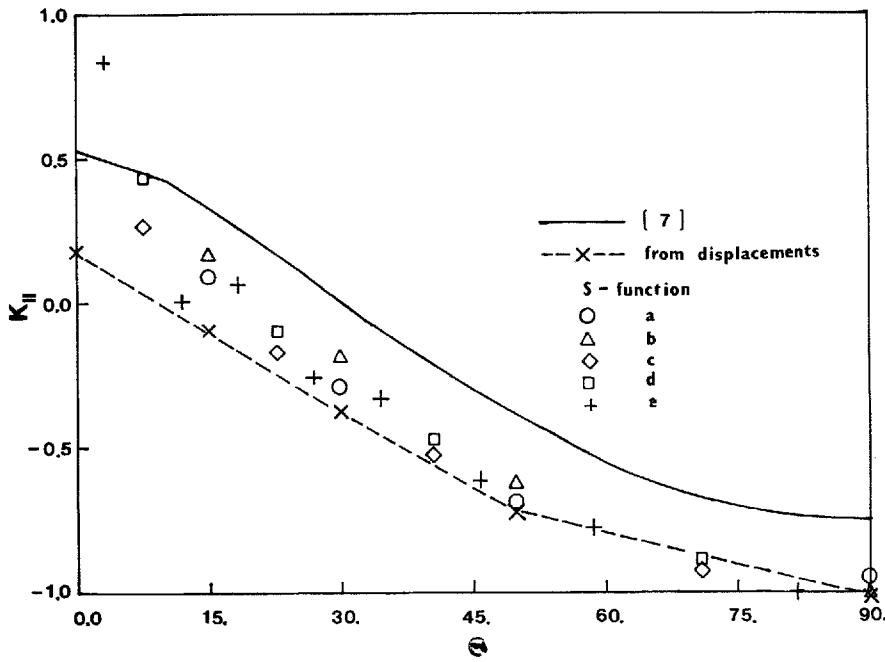

Figure 19. Results for normalized K_{II} for the problem of Figure 16

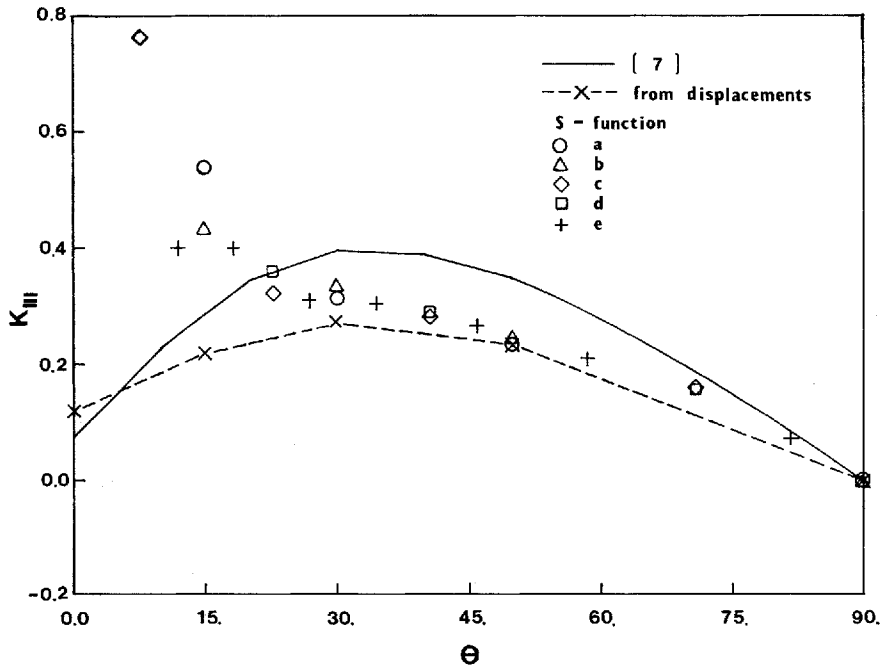

Figure 20. Results for normalized K_{III} for the problem of Figure 16, from computed J_1, J_2 and G_{III}

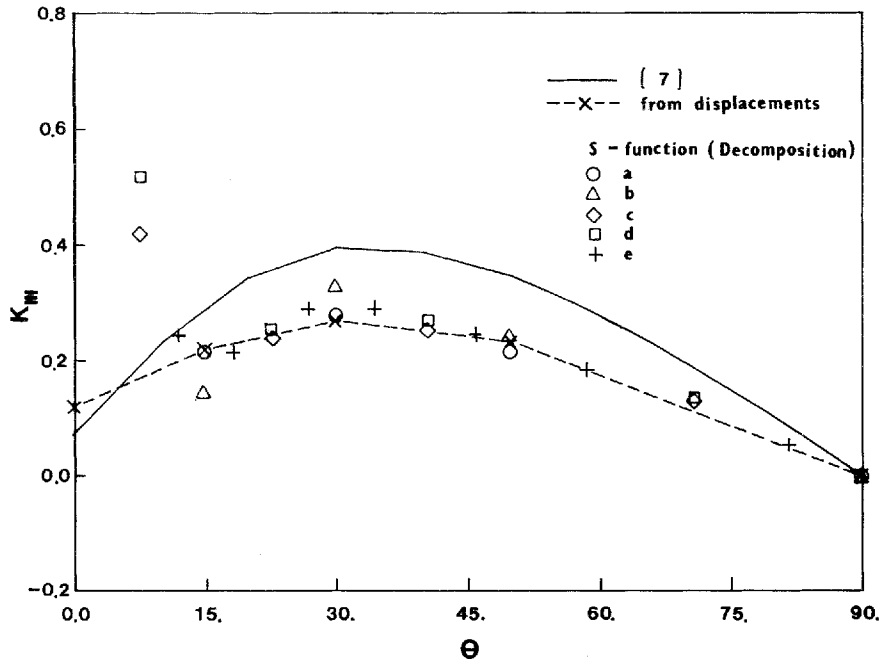

Figure 21. Results for normalized K_{III} for the problem of Figure 16, using the mode-decomposition method (G_I, G_{II} and G_{III})

where $K^{(1)}$ is the stress intensity factor at the quarter-point node, and $K^{(2)}$ is the stress intensity factor at the vertex node. The same procedure for the mode I crack problem was used by X. R. Wu.[18]

The analysis shows very good agreement of EDI results for the stress intensity factor K_I with the Benchmark solution.[17] Some differences of K_{II} and K_{III} values obtained by the EDI-method and in Reference 7 can be seen in Figures 19–21. Incorrect K_{III} values for small values of θ can be explained by the fact that the displacements u_2 and u_3 have the same sign on both surfaces of the crack for such angles. The situation can be improved by using decomposed displacements, strains and stresses (Figure 21). Errors may also be present due to the small values of K_{II} and K_{III} as compared to that of the K_I (the average shear stress τ is fifteen times less than the maximum normal stress, σ_{max}).

CLOSURE

A so-called 'equivalent domain integral' method which is analogous to the so-called 'virtual crack extension' method, *but which avoids the necessity of shifting the near-front nodes,* is presented for the evaluation of the *vector J*-integral along the front of an arbitrarily shaped three-dimensional crack in a structural component. The numerical algorithms necessary for the evaluation of the domain integrals have been given explicitly in the context of 20-noded brick finite elements. The numerical procedures that are presented in this paper remain valid for elastic–plastic materials when arbitrary histories of loading/unloading are considered.[19] Several numerical examples involving embedded as well as surface flaws of elliptical and part-elliptical shapes, respectively, are presented to illustrate the relative simplicity as well as the accuracy of the reported procedures.

In each example, the results obtained from the present simple procedures agree favorably with those reported in prior literature.

ACKNOWLEDGEMENTS

The first author thankfully acknowledges the financial support of the International Research & Exchanges Board, NY. The partial support of the office of Naval Research, and the encouragement of Dr. Y. Rajapakse are gratefully acknowledged. It is a pleasure to thank Ms. Cindi Anderson for her assistance in the preparation of the final typescript.

REFERENCES

1. K. Kishimoto, S. Aoki and M. Sakata, 'On the path-independent integral', *J. Eng. Fract. Mech.*, **13,** 841–850 (1980).
2. S. Aoki, K. Kishimoto and M. Sakata, 'Energy flux into process region in elastic-plastic fracture problems', *Eng. Fract. Mech.*, **19,** 827–836 (1984).
3. T. Murakami and T. Sato, 'Three-dimensional J-integral calculations of part-through surface crack problems', *Comp. Struct.*, **17,** 731–736 (1983).
4. H. G. Delorenzi, 'Energy release rate calculations by the finite element methods', *Eng. Fract. Mech.*, **21,** 129–143 (1985).
5. F. Z. Li, C. F. Shih and A. Needleman, 'A comparison of methods for calculating energy release rates', *Eng. Fract. Mech.*, **21,** 405–421 (1985).
6. T. Nishioka and S. N. Atluri, 'On the computation of mixed-mode K-factors for a dynamically propagating crack using path-independent integrals J_k', *Eng. Fract. Mech.*, **20,** 193–208 (1984).
7. H. L. Simon, P. E. O'Donoghue and S. N. Atluri, 'A finite element-alternating technique for evaluating mixed mode stress intensity factors for part-elliptical surface flaws', *Int. j. numer. methods eng.*, **24,** 689–709 (1987).
8. D. M. Parks, 'The virtual crack extension method for nonlinear material behaviour', *Computer Methods Appl. Mech. Eng.*, **12,** 353–364 (1977).
9. T. K. Hellen, 'On the method of virtual crack extension', *Int. j. numer. methods eng.*, **9,** 187–207 (1975).
10. G. P. Cherepanov, 'The propagation of cracks in a continuous medium', *J. Appl. Math. Mech.*, **31,** N3, 503–512 (1967).
11. J. R. Rice, 'A path independent integral and the approximate analysis of strain concentration by notches and cracks', *J. Appl. Mech. ASME*, **35,** 379–386 (1968).
12. G. P. Cherepanov, *Mechanics of Brittle Fracture*, McGraw-Hill, New York, 1979.
13. G. P. Nikishkov and V. A. Vainshtok, 'Method of virtual crack growth for determining stress intensity factors K_I and K_{II}', *Strength of Materials*, **12,** 696–701 (1980).
14. H. Ishikawa, 'A finite element analysis of stress intensity factors for combined tensile and shear loading by only a virtual crack extension', *Int. J. Fract.*, **16,** R243–R246 (1980).
15. G. T. Sha and C. T. Yang, 'Weight function calculations for mixed-node fracture problems with the virtual crack extension technique', *Eng. Fract. Mech.*, **21,** 1119–11150 (1985).
16. J. Barlow, 'Optimal stress locations in finite element models', *Int j. numer. methods eng.*, **10,** 243–251 (1976).
17. J. J. McGowan (ed.), *A Critical Evaluation of Numerical Solution to the 'Benchmark' Surface Flaw Problem. An Assessment of the Precision of Stress-Intensity Distributions for Surface Flaw Problems of Specified Geometry from Numerical Models and Comparison with Limited Experimental Results.* Benchmark Editorial Committee, SESA, 1980.
18. X. R. Wu, 'Stress intensity factors for half-elliptical surface cracks subjected to complex crack face loadings', *Eng. Fract. Mech.*, **19,** 387–405 (1984).
19. G. P. Nikishkov and S. N. Atluri, 'An 'equivalent domain integral' method for computing crack-tip integral parameters in non-elastic, thermomechanical fracture', *Eng. Fract. Mech.* (In Press).